scientific reports

OPEN

Comprehensive study of stochastic soliton solutions in nonlinear models with application to the Davey Stewartson equations

Yasir A. Madani[1], Shabbir Hussain[2], Mohammed A. Almalahi[3,4]✉, Blgys Muflh[5], Khaled A. Aldwoah[6]✉ & Mukhtar Y. Y. Abdalla[7]

This article investigates the stochastic Davey–Stewartson equations influenced by multiplicative noise within the framework of the Itô calculus. These equations are of significant importance because they extend the nonlinear Schrödinger equation into higher dimensions, serving as fundamental models for nonlinear phenomena in plasma physics, nonlinear optics, and hydrodynamics. This paper is motivated by the need to understand how random fluctuations affect soliton behavior in nonlinear systems. This is particularly relevant in applications such as turbulent plasma waves and optical fibers, where noise can significantly impact wave propagation. We employ the modified extended direct algebraic method for finding exact stochastic soliton solutions to the stochastic Davey–Stewartson equations. The study derives a class of exact stochastic soliton solutions, including dark, singular, rational, and periodic waves. MATLAB is used to provide visual representations of these stochastic soliton solutions through 3D surface plots, contour plots, and line plots. These solutions offer essential insights into how random disturbances influence nonlinear wave systems, particularly in turbulent plasma waves and optical fibers. To the best of our knowledge, the application of the modified extended direct algebraic method to the stochastic Davey–Stewartson equations with multiplicative noise, along with the subsequent analysis of the stabilizing effects on dark, singular, rational, and periodic stochastic soliton solutions is novel. The study demonstrates how multiplicative Brownian motion regulates these wave structures, providing new information on the impact of noise on higher-dimensional nonlinear systems.

Keywords DS-equations, Multiplicative noise, Stochastic soliton solutions, MEDA method, Dark soliton

The Davey–Stewartson equations are higher-dimensional generalizations of the nonlinear Schrödinger equation that are crucial models for a variety of non-linear phenomena in plasma physics, including nonlinear optics and hydrodynamics[1]. The impact of multiplicative noise on exact stochastic soliton solutions, especially using the modified extended direct algebraic method, has not been thoroughly investigated, although the deterministic Davey–Stewartson equations have been the topic of much research, and stochastic versions have been studied using a variety of numerical and analytical techniques. Researchers have not fully investigated how multiplicative Brownian motion affects stabilizing processes in dark, bright, rational, and periodic wave solutions of these equations. This paper fills the existing research gap through the application of a modified extended direct algebraic method to obtain exact stochastic soliton solutions for the Davey–Stewartson equations with multiplicative noise. The paper examines how multiplicative Brownian motion stabilizes dark, singular, rational, and periodic wave solutions. The research adds new analytical solutions along with insights into the complex noise-wave dynamics in higher-dimensional systems where multiplicative noise proves essential for stabilizing wave structures. The investigation under Itô calculus explores the stochastic DS equation which includes multiplicative noise[2–10]. In 1974, Davey and Stewartson developed the Davey–Stewartson equation (DSE). The DSE equation illustrates

[1]Department of Mathematics, College of Science, University of Ha'il, Ha'il 2440, Saudi Arabia. [2]Department of Mathematics and Statistics, University of Lahore, Lahore, Pakistan. [3]Department of Mathematics, College of Computer and Information Technology, Al-Razi University, Sana'a, Yemen. [4]Jadara University Research Center, Jadara University, Irbid, Jordan. [5]Department of Mathematics, College of Science and Humanities in Al-Kharj, Prince Sattam Bin Abdulaziz University, Al-Kharj 11942, Saudi Arabia. [6]Department of Mathematics, Faculty of Science, Islamic University of Madinah, Medinah 42351, Saudi Arabia. [7]Department of Mathematics, Faculty of Science, Taif University, Taif, Saudi Arabia. ✉email: dralmalahi@gmail.com; aldwoah@iu.edu.sa

the time-varying evolution of a three-dimensional wave packet in shallow water. Hydrodynamics, non-linear optics, plasma physics, and other disciplines have used the deterministic Davey–Stewartson equations (1) and (2), or $\sigma = 0$. For example, the interaction between microwaves and a properly matched spatio-temporal optical pattern may be explained by the DDSE solutions[11,12]. We consider the following Davey–Stewartson equations that are affected by multiplicative noise in the stochastic sense:[13]

$$i\Psi_t + \frac{1}{2}\alpha^2(\Psi_{xx} + \alpha^2\Psi_{yy}) + \lambda|\Psi|^2\Psi - \Phi\Psi + i\sigma\Psi\Xi_t = 0, \tag{1.1}$$

$$\Phi_{xx} - \alpha^2\Phi_{yy} - 2\lambda(|\Psi|^2)_{xx} = 0, \tag{1.2}$$

In Eqs. (1.1) and (1.2), $\Psi(x, y, t)$ represents the complex wave amplitude, while $\Phi(x, y, t)$ is a real-valued potential. The parameter α determines the type of Davey–Stewartson equation: $\alpha = 1$ corresponds to the DS-I equation, whereas $\alpha = i$ yields the DS-II equation[14–17]. The cubic non-linearity is governed by the constant λ, where $\lambda = +1$ and $\lambda = -1$ represent the focusing and defocusing cases, respectively. The noise intensity is denoted by σ, which scales the influence of the multiplicative noise term Ξ_t in the Itô sense, and it is the time derivative of Brownian motion $\Xi(t)$, that is, $\Xi_t = \dfrac{d\Xi}{dt}$ and $\Xi(t)$ is also called the standard Wiener process. It depends only on t[18]. Physically, the terms involving Ψ_{xx} and Ψ_{yy} represent dispersion in the x and y directions, respectively. The term involving Φ accounts for a self-induced potential, and the noise term $i\sigma\Psi\Xi_t$ represents the influence of random fluctuations on wave dynamics.

The stochastic DS-equations maintain integrability based on the characteristics of introduced stochastic noise and system nonlinearity. The deterministic DS-I and DS-II equations possess integrable solutions when specific conditions apply, whereas inverse scattering methods together with soliton and rational solutions become available. When Brownian motion serves as the multiplicative noise input the equations lose their integrability properties which hinders the application of inverse scattering transform methods. Most noise perturbations eliminate strict integrability but some specific noise structures or weak stochastic disturbances enable partial integrability and exact solutions. The noise characteristics determine whether integrable properties can be preserved because additive noise preserves integrability better than multiplicative noise. The MEDA method and other analytical approaches enable researchers to obtain exact or semi-analytical solutions even after full integrability is lost. Numerical methods including Monte Carlo simulations deliver important statistical data about solution behavior when studying stochastic systems. The analytical and numerical tractability of stochastic DS equations with multiplicative noise remains intact despite their lack of integrability properties.

The introduction of the Wiener process within our model is unique as it breaks away from deterministic definitions. It is possible to model structures changing over time using mathematical tools such as random processes, and the Wiener process in particular. This continuous-time stochastic process, which is utilised in stochastic calculus and has many applications in the social sciences, physical sciences, and quantitative finance, can be thought of as a continuous deformation of the fundamental random walk. This continuous-time stochastic process, which can be viewed as a continuous variation of the basic random walk, plays a crucial role in stochastic calculus and has found applications in diverse fields, from quantitative finance to physical sciences and social sciences. It makes possible to obtain the stochastic solutions in the sense of Itô calculus which is useful to study various processes like the formation of the ocean waves, the processes related to optical communication, the phenomena connected with the wave collapses in the astrophysics. We investigate the interplay between stochastic and random noise components and their link to physical properties to gain a better understanding of how these two types of factors affect wave behaviour.

Consider a Wiener process $\Xi(t)$ that is non-differentiable and has the following characteristics:[19,20]

$$\lim_{\Delta t \to 0} \Delta\Xi(t) = 0; \tag{1.3}$$

$$\lim_{\Delta t \to 0} \frac{(\Delta\Xi(_t))^N}{\Delta t} = \begin{cases} 1, & N = 2 \\ 0, & N = 3, 4, \ldots \end{cases} \tag{1.4}$$

A stochastic process $(\Xi_t)_{t \le 0}$ is said to be Brownian motion if the following criteria are met:

- Ξ_t is a continuous function for $t \le 0$.
- $\Xi_0 = 0$.
- For $t_1 < t_2$, $\Xi_{t_2} - \Xi_{t_1}$ is independent.
- $\Xi_{t_2} - \Xi_{t_1}$ has a normal distribution $\kappa(0, t_2 - t_1)$.

The fundamental nature of expectation lies at the core of probability theory as well as stochastic analysis when solving stochastic differential equations. Expectation enables analysis of average results obtained from multiple iterations of the random process. Stochastic wave equations require expectation to understand the statistical attributes of wave solutions which occur when noise act on them.[25–28] There have been several effective techniques suggested, including the new extended direct algebraic method[29], ϕ^6-expansion method[30], Hirota bilinear method[31–33], fractional modified Sardar subequation method and fractional enhanced modified extended tanh-expansion method[34], generalized exponential rational function method[35], generalized tanh-coth method[36], generalized Kudryashov method[37], improved $\tan(\frac{\phi}{2}$-expansion method[38], new modified exponential Jacobi technique[39] and so on. Here, we apply a powerful technique known as the modified extended direct algebraic method[40–43] to build a variety of exact soliton solutions for the nonlinear partial differential equation.

The modified extended direct algebraic method represents an effective method to solve nonlinear partial differential equations including stochastic Davey–Stewartson equations. This method delivers three main benefits which include exact solution-finding capabilities and efficient nonlinearity management and stochastic system compatibility that makes it ideal for practical usage. The method shows flexibility for use in plasma physics nonlinear optics and hydrodynamics because of its ability to analyze wave phenomena and soliton dynamics. The modified extended direct algebraic method delivers an improved understanding of random wave stabilization effects through its use of multiplicative noise, thus becoming an essential tool for studying stochastic wave systems

Algorithm for modified extended direct algebraic method

We provide the modified extended direct algebraic method[44–47] in this section. It is also referred to as the modified extended $\tanh$-function method[48–54]. The following steps outline the main steps in this technique, which we summarize here:

Suppose the following nonlinear partial differential equation

$$E(u, u_t, u_x, u_{tt}, u_{xx}, u_{xt}, \cdots) = 0, \tag{2.1}$$

E is a polynomial in $u = u(x,t)$ and its numerous partial derivatives, which involve nonlinear terms and the highest order derivatives, whereas $u = u(x,t)$ is a wave function.

Step 1. For wave solutions, apply the following wave transformation.

$$u = U(\zeta), \quad \zeta = x - v\,t. \tag{2.2}$$

where v is the wave speed.

Step 2. A nonlinear ordinary differential equation is obtained by plugging Eq. (2.2) into Eq. (2.1).

$$O(U, U', U'', U''', \cdots) = 0. \tag{2.3}$$

Step 3. Let $U(\zeta)$ be the next variable that can be expressed as a polynomial in $\eta(\zeta)$

$$U(\zeta) = B_0 + \sum_{i=1}^{M} B_i \eta^i + C_i \eta^{-i}, \tag{2.4}$$

where η' satisfies the nonlinear ODE, whereas there B_0, B_i, C_i, are unknown constants to be found later.

$$\eta' = \rho + \eta^2, \tag{2.5}$$

where ρ is an arbitrary constant, and $\eta' = \frac{d\eta}{d\zeta}$.

Step 4. Considering the homogeneous balance between the non-linear terms and the highest-order derivatives present in Eq. (2.3), one can deduce the value of the natural number M. To obtain a system of algebraic equations with respect to B_i, C_i, and ρ where $i = 1, 2, 3, \cdots M$, plug Eq. (2.4) into Eq. (2.2) and Eq. (2.5). At this stage, we shall determine B_0, B_i, C_i, ρ, and v since all the coefficients of η^i must vanish. The general solutions to Eq. (2.5) are as follows:

Family 1. If $\rho < 0$, we have

$$\eta(\zeta) = -\sqrt{-\rho}\tanh\left(\sqrt{-\rho}\zeta\right) \quad \text{or} \quad \eta(\zeta) = -\sqrt{-\rho}\coth\left(\sqrt{-\rho}\zeta\right). \tag{2.6}$$

Family 2. If $\rho > 0$, we have

$$\eta(\zeta) = \sqrt{\rho}\tan\left(\sqrt{\rho}\zeta\right) \quad \text{or} \quad \eta(\zeta) = -\sqrt{\rho}\cot\left(\sqrt{\rho}\zeta\right), \tag{2.7}$$

Family 3. If $\rho = 0$, we have

$$\eta(\zeta) = -\frac{1}{\zeta}. \tag{2.8}$$

Application of the Davey–Stewartson equations affected by multiplicative noise in the Itô calculus sense

Making stochastic wave transformation for Eqs. (1.1) and (1.2)

$$\Psi(x,y,t) = U(\zeta)e^{(i\Omega - \sigma\Xi(t) - \sigma^2 t)}, \quad \Phi(x,y,t) = V(\zeta)e^{-2\sigma\Xi(t) - 2\sigma^2 t}, \tag{3.1}$$

with

$$\zeta = \zeta_1 x + \zeta_2 y - \zeta_3 t, \quad \text{and} \quad \Omega = kx + wy + \theta t,$$

where ζ, Ω are deterministic functions and $\{\zeta_1, \zeta_2, \zeta_3\}$, $\{k, w, \theta\}$ are nonzero constants. Putting Eq. (3.1) into Eq. (1.1) and Eq. (1.2) respectively, then we obtain for the real part

$$\left(\frac{1}{2}\zeta_1^2\alpha^2 + \frac{1}{2}\zeta_2^2\alpha^4\right)U'' - \left(\theta + \frac{1}{2}\alpha^2k^2 + \frac{1}{2}\alpha^4w^2\right)U + \left(kU^3 - UV\right)e^{(-2\sigma\Xi(t)-2\sigma^2t)} = 0, \tag{3.2}$$

$$\left(\zeta_1^2 - \alpha^2\zeta_2^2\right)V'' - 2\zeta_1k(U^2)'' = 0, \tag{3.3}$$

and, imaginary part,

$$(-\zeta_3 + 2\zeta_1k + 2\zeta_2w)\,U' = 0. \tag{3.4}$$

From Eq. (3.4), we obtain

$$\zeta_3 = 2\zeta_1k + 2\zeta_2w. \tag{3.5}$$

Now, integrating Eq. (3.3) once, we attain

$$V = \frac{2\zeta_1^2k}{(\zeta_1^2 - \alpha^2\zeta_2^2)}U^2. \tag{3.6}$$

Substituting Eq. (3.6) into Eq. (3.2) , we obtain

$$U'' - \mu_2U + \mu_1U^3e^{-2\sigma\Xi(t)-2\sigma^2t} = 0, \tag{3.7}$$

where

$$\mu_1 = \frac{2\lambda}{\alpha^2(\zeta_1^2 - \alpha^2\zeta_2^2)},\ \mu_2 = \frac{2\theta + \alpha^2k^2 + \alpha^4w^2}{\zeta_1^2\alpha^2 + \zeta_2^2\alpha^4},\ \mu_3 = \frac{2\zeta_1^2k}{(\zeta_1^2 - \alpha^2\zeta_2^2)}. \tag{3.8}$$

We take the expectation on both sides

$$U'' - \mu_2U - \mu_1U^3e^{-2\sigma^2t}E\left(e^{-2\sigma\Xi(t)}\right) = 0. \tag{3.9}$$

Since $\Xi(t)$ is normally distributed, so $E\left(e^{-2\sigma\Xi(t)}\right) = e^{2\sigma^2t}$. Hence, Eq. (3.9) becomes

$$U'' - \mu_1U^3 - \mu_2U = 0. \tag{3.10}$$

Balancing the highest degree derivative U'' along with the nonlinear term U^3 in Eq. (3.10), we obtain $M = 1$. Hence the formal solution of Eq. (3.10) is

$$U(\zeta) = \beta_0 + \beta_1\eta(\zeta) + \frac{\beta_2}{\eta(\zeta)} \tag{3.11}$$

Plugging Eq. (3.11) along with Eq. (2.5) into Eq. (3.10) will provide these constants, as well as collecting all terms with the same power of $\eta^i, i = 0, 1, \cdots, M$ and setting every coefficient equal to zero, hence the following collection of algebraic equations is obtained

$$\begin{cases} -\mu_1\beta_1^3 + 2\beta_1 & = 0, \\ -3\mu_1\beta_1^2 + \beta_2 - \mu_2\beta_1 + 2\beta_1\rho - 3\mu_1\beta_0^2\beta_1 & = 0, \\ -\mu_2\beta_0 - \mu_1\beta_0^3 - 6\mu_1\beta_0\beta_1\beta_2 & = 0, \\ -3\mu_1\beta_0^2\beta_2 + 2\beta_2\rho - \mu_2\beta_2 - 3\mu_1\beta_1\beta_2^2 & = 0, \\ 2\beta_2\rho^2 - \mu_1\beta_2^3 & = 0. \end{cases} \tag{3.12}$$

The following set of solutions are possible for solving the (3.12) using Maple.

Case I. If $\beta_2 = 0$ then (3.12) gives: $\beta_0 = \frac{\sqrt{-\mu_1\mu_2}}{\mu_1}$, $\beta_1 = \pm\frac{\sqrt{2}}{\sqrt{\mu_1}}$.

Case II. If $\beta_0 = 0$ then (3.12) gives: $\beta_1 = \pm\frac{\sqrt{2}}{\sqrt{\mu_1}}$, $\beta_2 = \frac{2\rho-\alpha_2}{3\sqrt{\mu_1}}$.

Case III. If $\beta_1 = 0$ then (3.12) gives: $\beta_2 = \pm\frac{\sqrt{2}\rho}{\sqrt{\mu_1}}$, $\beta_0 = \pm\frac{1}{\sqrt{3}}\frac{\sqrt{\mu_1(2\rho-\mu_2)}}{\mu_1}$.

Using cases I, II, and III, we can obtain the following stochastic soliton solutions.

Case (I)

Family (I) provides the following dark (Ψ_1,Φ_1) and singular (Ψ_2,Φ_2) stochastic soliton solitons for $\rho < 0$,

$$\Psi_1 = \left[\pm\frac{\sqrt{-\mu_1\mu_2}}{\mu_1} \pm \frac{\sqrt{2}}{\sqrt{\mu_1}}\left(-\sqrt{-\rho}\tanh\left(\sqrt{-\rho}\zeta\right)\right)\right]e^{(i(kx+wy+\theta t)-\sigma\Xi(t)-\sigma^2t)},$$

or

$$\Psi_2=\left[\pm\frac{\sqrt{-\mu_1\mu_2}}{\mu_1}\pm\frac{\sqrt{2}}{\sqrt{\mu_1}}\left(-\sqrt{-\rho}\coth\left(\sqrt{-\rho}\zeta\right)\right)\right]e^{(i(kx+wy+\theta t)-\sigma\Xi(t)-\sigma^2 t)},$$

and

$$\Phi_1=\mu_3\left(\left[\pm\frac{\sqrt{-\mu_1\mu_2}}{\mu_1}\pm\frac{\sqrt{2}}{\sqrt{\mu_1}}\left(-\sqrt{-\rho}\tanh\left(\sqrt{-\rho}\zeta\right)\right)\right]\right)^2 e^{-2\sigma\Xi(t)-2\sigma^2 t},$$

or

$$\Phi_2=\mu_3\left(\left[\pm\frac{\sqrt{-\mu_1\mu_2}}{\mu_1}\pm\frac{\sqrt{2}}{\sqrt{\mu_1}}\left(-\sqrt{-\rho}\coth\left(\sqrt{-\rho}\zeta\right)\right)\right]\right)^2 e^{-2\sigma\Xi(t)-2\sigma^2 t}.$$

Family (II) provides the following (Ψ_3,Φ_3, Ψ_4,Φ_4) periodic stochastic soliton solitons for $\rho>0$,

$$\Psi_3=\left[\pm\frac{\sqrt{-\mu_1\mu_2}}{\mu_1}\pm\frac{\sqrt{2}}{\sqrt{\mu_1}}\left(\sqrt{\rho}\tan\left(\sqrt{\rho}\zeta\right)\right)\right]e^{(i(kx+wy+\theta t)-\sigma\Xi(t)-\sigma^2 t)},$$

or

$$\Psi_4=\left[\pm\frac{\sqrt{-\mu_1\mu_2}}{\mu_1}\pm\frac{\sqrt{2}}{\sqrt{\mu_1}}\left(-\sqrt{\rho}\cot\left(\sqrt{\rho}\zeta\right)\right)\right]e^{(i(kx+wy+\theta t)-\sigma\Xi(t)-\sigma^2 t)},$$

and

$$\Phi_3=\mu_3\left(\left[\pm\frac{\sqrt{-\mu_1\mu_2}}{\mu_1}\pm\frac{\sqrt{2}}{\sqrt{\mu_1}}\left(\sqrt{\rho}\tan\left(\sqrt{\rho}\zeta\right)\right)\right]\right)^2 e^{-2\sigma\Xi(t)-2\sigma^2 t},$$

or

$$\Phi_4=\mu_3\left(\left[\pm\frac{\sqrt{-\mu_1\mu_2}}{\mu_1}\pm\frac{\sqrt{2}}{\sqrt{\mu_1}}\left(-\sqrt{\rho}\cot\left(\sqrt{\rho}\zeta\right)\right)\right]\right)^2 e^{-2\sigma\Xi(t)-2\sigma^2 t}.$$

Family (III) provides the following (Ψ_5,Φ_5) rational stochastic soliton solitons for $\rho=0$,

$$\Psi_5=\left[\pm\frac{\sqrt{-\mu_1\mu_2}}{\mu_1}\pm\frac{\sqrt{2}}{\sqrt{\mu_1}}\left(-\frac{1}{\zeta}\right)\right]e^{(i(kx+wy+\theta t)-\sigma\Xi(t)-\sigma^2 t)},$$
$$\Phi_5=\mu_3\left(\left[\pm\frac{\sqrt{-\mu_1\mu_2}}{\mu_1}\pm\frac{\sqrt{2}}{\sqrt{\mu_1}}\left(-\frac{1}{\zeta}\right)\right]\right)^2 e^{-2\sigma\Xi(t)-2\sigma^2 t},$$

Case (II)

Family (I) provides the following dark (Ψ_6,Φ_6) and singular (Ψ_7,Φ_7) stochastic soliton solitons for $\rho<0$,

$$\Psi_6=\left[\pm\frac{\sqrt{2}}{\sqrt{\mu_1}}\left(-\sqrt{-\rho}\tanh\left(\sqrt{-\rho}z\right)\right)\pm\frac{2\,c-\mu_2}{3\sqrt{\mu_1}}\left(\sqrt{-\rho}\tanh\left(\sqrt{-\rho}\zeta\right)\right)^{-1}\right]e^{(i(kx+wy+\theta t)-\sigma\Xi(t)-\sigma^2 t)},$$

or

$$\Psi_7=\left[\pm\frac{\sqrt{2}}{\sqrt{\mu_1}}\left(-\sqrt{-\rho}\coth\left(\sqrt{-\rho}z\right)\right)\pm\frac{2\,c-\mu_2}{3\sqrt{\mu_1}}\left(-\sqrt{-\rho}\coth\left(\sqrt{-\rho}\zeta\right)\right)^{-1}\right]e^{(i(kx+wy+\theta t)-\sigma\Xi(t)-\sigma^2 t)},$$

and

$$\Phi_6=\mu_3\left(\left[\pm\frac{\sqrt{2}}{\sqrt{\mu_1}}\left(-\sqrt{-\rho}\tanh\left(\sqrt{-\rho}z\right)\right)\pm\frac{2\,c-\mu_2}{3\sqrt{\mu_1}}\left(\sqrt{-\rho}\tanh\left(\sqrt{-\rho}\zeta\right)\right)^{-1}\right]\right)^2 e^{-2\sigma\Xi(t)-2\sigma^2 t},$$

or

$$\Phi_7=\mu_3\left(\left[\pm\frac{\sqrt{2}}{\sqrt{\mu_1}}\left(-\sqrt{-\rho}\coth\left(\sqrt{-\rho}z\right)\right)\pm\frac{2\,c-\mu_2}{3\sqrt{\mu_1}}\left(-\sqrt{-\rho}\coth\left(\sqrt{-\rho}\zeta\right)\right)^{-1}\right]\right)^2 e^{-2\sigma\Xi(t)-2\sigma^2 t}.$$

Family (II) provides the following (Ψ_8,Φ_8, Ψ_9,Φ_9) periodic stochastic soliton solitons for $\rho > 0$,

$$\Psi_8 = \left[\pm \frac{\sqrt{2}}{\sqrt{\mu_1}} \left(\sqrt{\rho} \tan\left(\sqrt{\rho}\zeta\right)\right) \pm \frac{2\,c - \mu_2}{3\sqrt{\mu_1}} \left(\sqrt{\rho} \tan\left(\sqrt{\rho}\zeta\right)\right)^{-1} \right] e^{(i(kx+wy+\theta t)-\sigma \Xi(t)-\sigma^2 t)},$$

or

$$\Psi_9 = \left[\pm \frac{\sqrt{2}}{\sqrt{\mu_1}} \left(-\sqrt{\rho} \cot\left(\sqrt{\rho}\zeta\right)\right) \pm \frac{2\,c - \mu_2}{3\sqrt{\mu_1}} \left(-\sqrt{\rho} \cot\left(\sqrt{\rho}\zeta\right)\right)^{-1} \right] e^{(i(kx+wy+\theta t)-\sigma \Xi(t)-\sigma^2 t)},$$

and

$$\Phi_8 = \mu_3 \left(\left[\pm \frac{\sqrt{2}}{\sqrt{\mu_1}} \left(\sqrt{\rho} \tan\left(\sqrt{\rho}\zeta\right)\right) \pm \frac{2\,c - \mu_2}{3\sqrt{\mu_1}} \left(\sqrt{\rho} \tan\left(\sqrt{\rho}\zeta\right)\right)^{-1} \right] \right)^2,$$

or

$$\Phi_9 = \mu_3 \left(\left[\pm \frac{\sqrt{2}}{\sqrt{\mu_1}} \left(-\sqrt{\rho} \cot\left(\sqrt{\rho}\zeta\right)\right) \pm \frac{2\,c - \mu_2}{3\sqrt{\mu_1}} \left(-\sqrt{\rho} \cot\left(\sqrt{\rho}\zeta\right)\right)^{-1} \right] e^{-2\sigma \Xi(t)-2\sigma^2 t} \right)^2,$$

Family (III) provides the following (Ψ_{10},Φ_{10}) rational stochastic soliton solitons for $\rho = 0$,

$$\Psi_{10} = \left[\pm \frac{\sqrt{2}}{\sqrt{\mu_1}} \left(-\frac{1}{\zeta}\right) \pm \frac{2\,c - \mu_2}{3\sqrt{\mu_1}} \left(-\frac{1}{\zeta}\right)^{-1} \right] e^{(i(kx+wy+\theta t)-\sigma \Xi(t)-\sigma^2 t)},$$

$$\Phi_{10} = \mu_3 \left(\left[\pm \frac{\sqrt{2}}{\sqrt{\mu_1}} \left(-\frac{1}{\zeta}\right) \pm \frac{2\,c - \mu_2}{3\sqrt{\mu_1}} \left(-\frac{1}{\zeta}\right)^{-1} \right] \right)^2 e^{-2\sigma \Xi(t)-2\sigma^2 t}.$$

Case (III)

Family (I) provides the following dark (Ψ_{11},Φ_{11}) and singular (Ψ_{12},Φ_{12}) stochastic soliton solitons for $\rho < 0$,

$$\Psi_{11} = \left[\frac{1}{\sqrt{3}} \frac{\sqrt{\mu_1(2\rho - \mu_2)}}{\mu_1} \pm \frac{-\sqrt{2}\,c}{\sqrt{\mu_1}} \left(-\sqrt{-\rho} \tanh\left(\sqrt{-\rho}\zeta\right)\right)^{-1} \right] e^{(i(kx+wy+\theta t)-\sigma \Xi(t)-\sigma^2 t)},$$

or

$$\Psi_{12} = \left[\frac{1}{\sqrt{3}} \frac{\sqrt{\mu_1(2\rho - \mu_2)}}{\mu_1} \pm \frac{-\sqrt{2}\,c}{\sqrt{\mu_1}} \left(-\sqrt{-\rho} \coth\left(\sqrt{-\rho}\zeta\right)\right)^{-1} \right] e^{(i(kx+wy+\theta t)-\sigma \Xi(t)-\sigma^2 t)},$$

$$\Phi_{11} = \mu_3 \left(\left[\frac{1}{\sqrt{3}} \frac{\sqrt{\mu_1(2\rho - \mu_2)}}{\mu_1} \pm \frac{-\sqrt{2}\,c}{\sqrt{\mu_1}} \left(-\sqrt{-\rho} \tanh\left(\sqrt{-\rho}\zeta\right)\right)^{-1} \right] \right)^2 e^{-2\sigma \Xi(t)-2\sigma^2 t},$$

or

$$\Phi_{12} = \mu_3 \left(\left[\frac{1}{\sqrt{3}} \frac{\sqrt{\mu_1(2\rho - \mu_2)}}{\mu_1} \pm \frac{-\sqrt{2}\,c}{\sqrt{\mu_1}} \left(-\sqrt{-\rho} \coth\left(\sqrt{-\rho}\zeta\right)\right)^{-1} \right] \right)^2 e^{-2\sigma \Xi(t)-2\sigma^2 t}.$$

Family (II) provides the following (Ψ_{13},Φ_{13}, Ψ_{14},Φ_{14}) periodic stochastic soliton solitons for $\rho > 0$,

$$\Psi_{13} = \left[\frac{1}{\sqrt{3}} \frac{\sqrt{\mu_1(2\rho - \mu_2)}}{\mu_1} \pm \frac{-\sqrt{2}\,c}{\sqrt{\mu_1}} \left(\sqrt{\rho} \tan\left(\sqrt{\rho}\zeta\right)\right)^{-1} \right] e^{(i(kx+wy+\theta t)-\sigma \Xi(t)-\sigma^2 t)},$$

or

$$\Psi_{14} = \left[\frac{1}{\sqrt{3}} \frac{\sqrt{\mu_1(2\rho - \mu_2)}}{\mu_1} \pm \frac{-\sqrt{2}\,c}{\sqrt{\mu_1}} \left(-\sqrt{\rho} \cot\left(\sqrt{\rho}\zeta\right)\right)^{-1} \right] e^{(i(kx+wy+\theta t)-\sigma \Xi(t)-\sigma^2 t)},$$

$$\Phi_{13} = \mu_3 \left(\left[\frac{1}{\sqrt{3}} \frac{\sqrt{\mu_1(2\rho - \mu_2)}}{\mu_1} \pm \frac{-\sqrt{2}\,c}{\sqrt{\mu_1}} \left(\sqrt{\rho} \tan\left(\sqrt{\rho}\zeta\right)\right)^{-1} \right] \right)^2 e^{-2\sigma \Xi(t)-2\sigma^2 t},$$

or

$$\Phi_{14} = \mu_3 \left(\left[\frac{1}{\sqrt{3}} \frac{\sqrt{\mu_1(2\rho - \mu_2)}}{\mu_1} \pm \frac{-\sqrt{2}\,c}{\sqrt{\mu_1}} \left(-\sqrt{\rho} \cot\left(\sqrt{\rho}\zeta\right) \right)^{-1} \right] \right)^2 e^{-2\sigma\Xi(t) - 2\sigma^2 t}.$$

Family (III) provides the following (Ψ_{15},Φ_{15}) rational stochastic soliton solitons for $\rho = 0$,

$$\Psi_{15} = \left[\pm \frac{1}{\sqrt{3}} \frac{\sqrt{\mu_1(2\rho - \mu_2)}}{\mu_1} \pm \frac{-\sqrt{2}\,c}{\sqrt{\mu_1}} \left(-\frac{1}{\zeta} \right)^{-1} \right] e^{(i(kx+wy+\theta t) - \sigma\Xi(t) - \sigma^2 t)},$$

$$\Phi_{15} = \mu_3 \left(\left[\pm \frac{1}{\sqrt{3}} \frac{\sqrt{\mu_1(2\rho - \mu_2)}}{\mu_1} \pm \frac{-\sqrt{2}\,c}{\sqrt{\mu_1}} \left(-\frac{1}{\zeta} \right)^{-1} \right] \right)^2 e^{-2\sigma\Xi(t) - 2\sigma^2 t}.$$

The graphical representation

To visualize and analyze the impact of noise, MATLAB tool has been employed to plot the three-dimensional, two-dimensional as well as contour plots of the obtained solutions. These plots give a better picture of how solitons respond to under the various noise intensities. The waveforms are plotted in 3 dimensions in order to reveal the temporal and spatial changes and how they converge to be stable around the zero. Two-dimensional cross-sections bring out the amplitude variations clearly; contour maps provide a better view of structure of the wave and variation of intensity.

Results and discussion

This section of our work consists of the results and a literary comparison. The classical Davey–Stewartson (DS) equation which Davey and Stewartson developed in 1974 underwent extensive research in recent years. Through their work Yan et al.[55] discovered high-order lump solutions of the DS model while Behera and Virdi[56] deployed the $\frac{G'}{G}$ -model expansion method to obtain soliton solutions. Ding et al.[57] studied dark and anti-dark solitons whereas Coppini et al.[58] developed N-breather anomalous wave solutions. The analysis of Lie point symmetries together with similarity reductions and conservation laws for the DS equation appears in Guo et al.[59]. Liu and Li[60] analyzed the DS equation as it interacted with time-noise effects at the multiplicative level. The research examines the stochastic Davey–Stewartson (SDS) equation through the application of the MEDA method to discover diverse exact stochastic soliton solutions. Using this approach we obtained diverse solution types such as dark ones as well as trigonometric ones, rational solutions, and periodic wave solutions. We investigate multiple physical consequences of noise on these solutions. We use MATLAB software to draw graphical representations of soliton solutions which show how they act with varying noise strength. Our findings yield traditional stochastic soliton solutions of the DS equation as the noise parameter reaches zero value. These findings serve to advance dynamical systems research in noisy conditions by offering important observations regarding future investigation.

Physical interpretation

A dark stochastic soliton is a soliton that moves in a nonlinear dispersive medium that contains fluctuations or random noise. Even if random influences vary the position, depth, phase, etc. of these solitons, they do not significantly change their general form of localized dip on a continuous wave background. On a continuous wave background, they occur in localized dips, although random variables might cause variations in their characteristics (position, depth, or phase). With a focus on how these solitons behave to stochastic perturbations, they are studied in systems where a random character is inherent, such as optical fibers, Bose-Einstein Condensates etc. Multiplicative noise introduces random disturbances to amplitudes, depths, phases, and positions, which can disrupt the soliton's localised dip and deform dark stochastic solitons. Soliton broadening, energy exchange with the background, or a transition to chaotic dynamics under high noise intensities. These effects are important for investigations of soliton stability in stochastically nonlinear media. A periodic stochastic soliton undergoes random perturbations that periodically alter its amplitude, phase, or velocity, among other properties. They are studied in fields like optical communications, quantum fluids, and plasma physics; often, stochastic effects necessitate the use of analytical solutions. They are typically represented by stochastic nonlinear partial differential equations as the nonlinear Schrödinger equation with noise. A stochastic soliton solution of rational type is one in which the soliton is represented by rational functions, with a profile consisting of a ratio of functions. It differs from conventional exponential or trigonometric soliton solutions in that it uses stochastic variables for building algebraic patterns. Figures 1, 6, 10, 15, 20, and 25 display dark stochastic soliton solutions while Figs. 2, 7, 11, 16, 21 and 26 display singular stochastic soliton solutions. Similarly Figs. 3, 4, 8, 12, 13, 17, 18, 22, 23, 27, and 28 display periodic stochastic soliton solutions. Furthermore the Figs. 5, 9, 14, 19, 24, and 29 display rational stochastic soliton solutions.

In conclusion, all figures pertaining to dark, singular, periodic, and rational solitons in different kinds of plots are essential tools to investigate nonlinear systems. They are employed to illustrate underlying patterns in situations where it is difficult to recognise new connections; practically, they support research goals in domains ranging from plasma physics to quantum mechanics and optics by providing reasoning, prediction, and validation for new ideas. The observations show that multiplicative noise creates various impacts on dark, periodic and rational solitons across multiple ways. The soliton starts to disperse due to the introduced dispersive effects which lead to its reduced localization. The bright peak along with the dark dip becomes increasingly wider due to this effect. The combination of noise with other factors reduces the amplitude levels of bright as

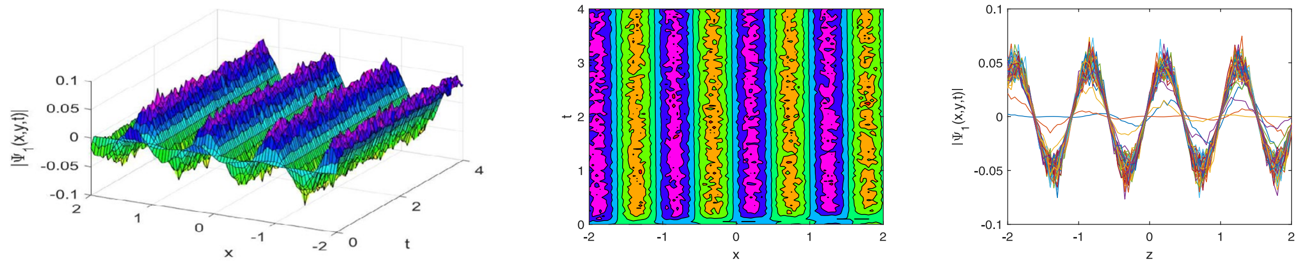

(a) (b) (c)

Fig. 1. (Matlab R2017a (9.2.0.538062)) The 3 dim, contour and line plots of $|\Psi_1(x, y, t)|$ for $\sigma = 0.08, \zeta_1 = 0.5, \zeta_2 = 0.7, w = 8.7, k = 3, \lambda = 0.25, \theta = 0.2, \rho = -0.5, y = 1, z = 0$, and $\Xi(t) =$ randn.

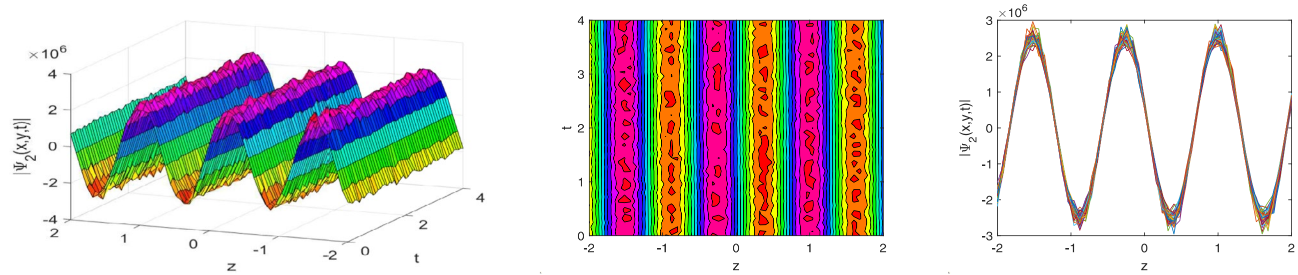

(a) (b) (c)

Fig. 2. (Matlab R2017a (9.2.0.538062)) The 3 dim, contour and line plots of $|\Psi_2(x, y, t)|$ for $\sigma = 0.08, \zeta_1 = 0.5, \zeta_2 = 0.7, w = 8.7, k = 3, \lambda = 0.25, \theta = 0.2, \rho = -0.5, y = 1, z = 0$, and $\Xi(t)$randn.

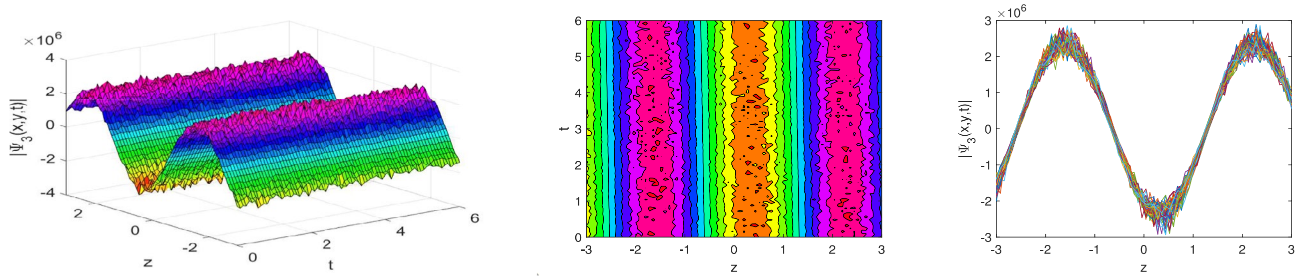

(a) (b) (c)

Fig. 3. (Matlab R2017a (9.2.0.538062))The 3 dim, contour and line plots of $|\Psi_3(x, y, t)|$ for $\sigma = 0.08, \zeta_1 = 0.15, \zeta_2 = 1.7, w = 5.7, k = 1.63, \lambda = 10.25, \theta = 0.2, \rho = 125.5, y = 1, z = 0$, and $\Xi(t)$ randn.

well as dark components thus weakening the soliton structure fundamentally. The transmission of noise causes structural definition loss which makes bright-dark area boundaries fade into each other in the optical field. The delicate nonlinear balance needed for sustaining the soliton's shape becomes disturbed by random fluctuations that arise from noise-induced perturbations. Noise drives unnecessary distribution of energy that pulls away from the localized soliton structure which then results in its deterioration. The effects demonstrate why noise plays such an important part in controlling the stability and movement patterns of soliton solutions.

Conclusion

We studied the stochastic Davey–Stewartson equations which serve as a fundamental tool for studying complex wave phenomena in environments affected by noise. The MEDA method provided exact stochastic soliton solutions which included bright, dark, singular, rational and periodic waveforms. The mathematical simulations showed that Brownian motion which models multiplicative noise causes major modifications to the solutions that lead toward zero-stabilization as their primary outcome. MATLAB-generated graphical

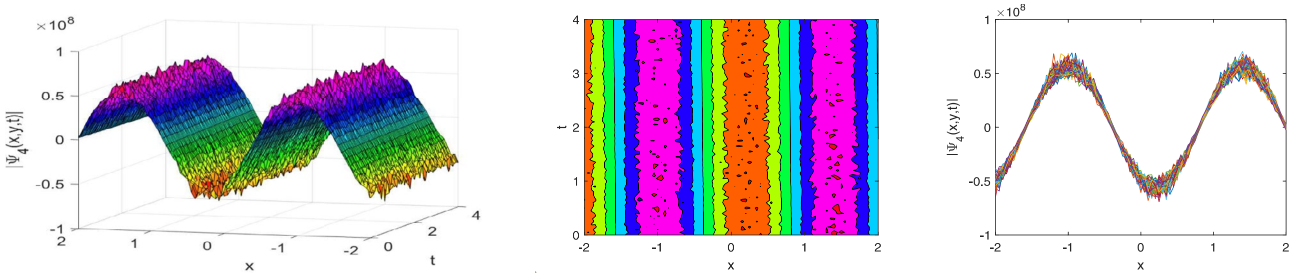

(a) (b) (c)

Fig. 4. (Matlab R2017a (9.2.0.538062)) The 3 dim, contour and line plots of $|\Psi_4\,(x, y, t)\,|$ for $\sigma = 0.09, \zeta_1 = 0.15, \zeta_2 = 1.7, w5.7, k = 2.63, \lambda = 20.25, \theta = 0.02, \rho = 2.06, y = 1, z = 0$, and $\Xi(t)$ randn.

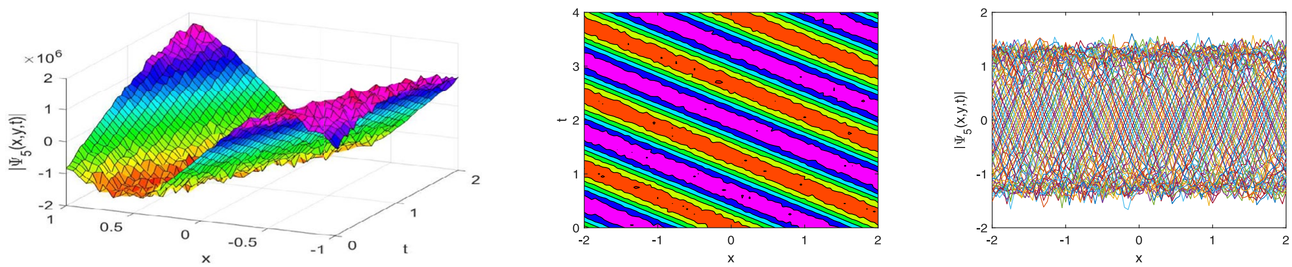

(a) (b) (c)

Fig. 5. (Matlab R2017a (9.2.0.538062)) The 3 dim, contour and line plots of $|\Psi_5\,(x, y, t)\,|$ for $\sigma = 0.08, \zeta_1 = 0.15, \zeta_2 = 1.7, w4.7, k = 2.63, \lambda = 10.25, \theta = 1.02, \rho = 0, y = 1, z = 0$, and $\Xi(t) =$ randn.

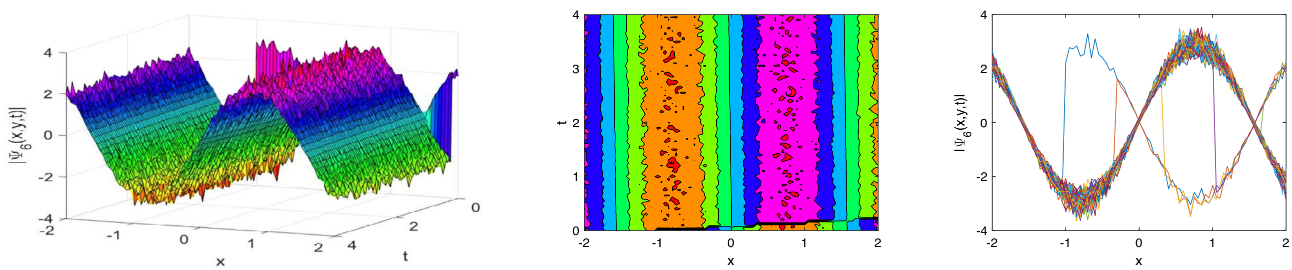

(a) (b) (c)

Fig. 6. (Matlab R2017a (9.2.0.538062)) The 3 dim, contour and line plots of $|\Psi_6\,(x, y, t)\,|$ $\sigma = 0.09, \zeta_1 = 10.5, \zeta_2 = 10.7, w = 4.7, k = 2, \lambda = 0.25, \theta = 0.02, \rho = -98825.5, y = 1, z = 0$, and $\Xi(t)$ =randn.

analysis demonstrates the detailed relationship of noise with nonlinear wave patterns effectively. Such findings generate ramifications that enhance our knowledge about noisily driven wave phenomena across the fields of plasma physics and nonlinear optics alongside fluid dynamics of complex systems. The field benefits from this research which offers an essential fundamental view of randomness effects on soliton motion by surpassing the current perturbative and numerical methods. Multiplicative noise produces observed wave stabilization effects indicating a potential process for noise-driven order which might lead to practical wave structure control within stochastic systems. The construction of exact stochastic solutions in this work provides an essential basis which supports future investigations of wave propagation under random disturbances. Related works studied stochastic NLS and DS equations yet they withheld the approach for developing exact stochastic soliton solutions of Davey–Stewartson equations with multiplicative noise through MEDA methodology. Future investigations should analyze more progressive noise models beyond white noise using fractional Brownian motion together with colored noise since they better reproduce diverse stochastic processes. The investigation of control methods which strengthen soliton stability under random external disturbances shows potential for practical realization.

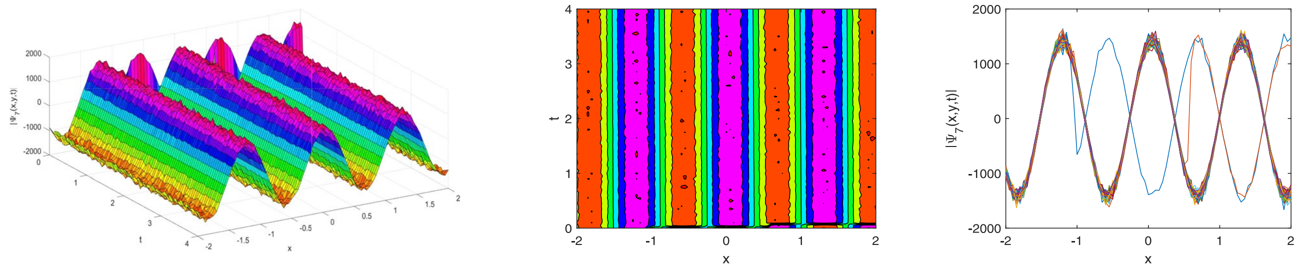

(a) (b) (c)

Fig. 7. (Matlab R2017a (9.2.0.538062)) The 3 dim, contour and line plots of $|\Psi_7(x,y,t)|$ $\sigma = 0.05, \zeta_1 = 10.4, \zeta_2 = 10.8, w = 10.7, k = 5, \lambda = 2.25, \theta = 0.02, \rho = -10.5, y = 1, z = 0$, and $\Xi(t) =$randn.

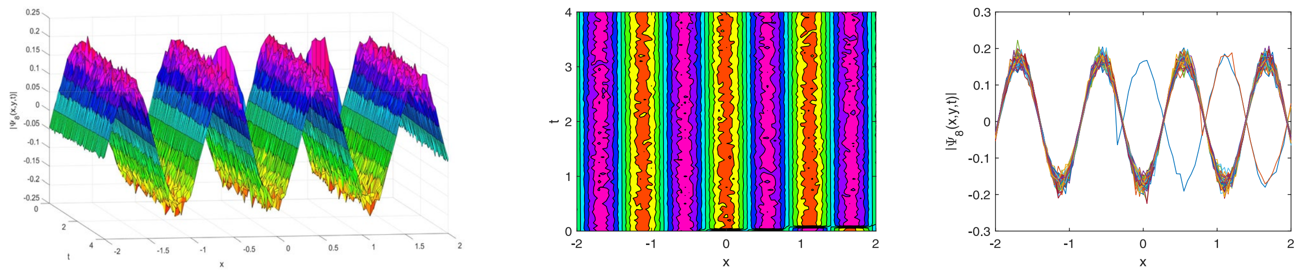

(a) (b) (c)

Fig. 8. (Matlab R2017a (9.2.0.538062)) The 3 dim, contour and line plots of $|\Psi_8(x,y,t)|$ $\sigma = 0.09, \zeta_1 = 10.15, \zeta_2 = 3.7, w = 15.7, k = 5.63, \lambda = 0.025, \theta = 0.02, \rho = 98800, y = 1, z = 0$, and $\Xi(t) =$randn.

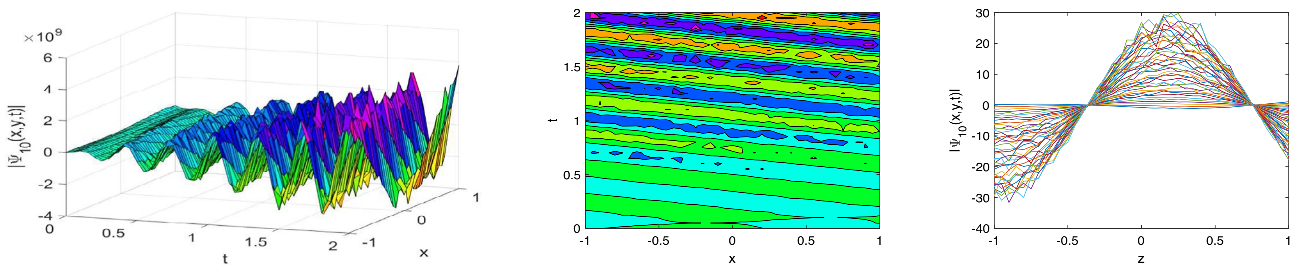

(a) (b) (c)

Fig. 9. (Matlab R2017a (9.2.0.538062)) The 3 dim, contour and line plots of $|\Psi_{10}(x,y,t)|$ $\sigma = 0.16, \zeta_1 = 2.4, \zeta_2 = 2.8, w = 5.7, k = 2.8, \lambda = 5.25, \theta = 20.02, \rho = 0y = 1, z = 0$, and $\Xi(t) =$randn.

Exact stochastic solutions derived in this work function as reference points for verifying numerical methods while helping in developing stable control strategies for noisy nonlinear systems. Future investigations should apply the discovered stochastic soliton solutions to actual situations involving optical fiber communication and wave propagation through turbulent plasmas.

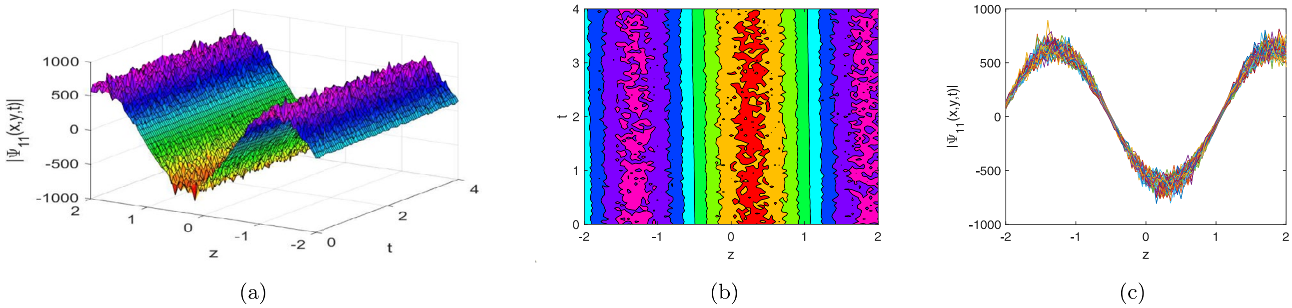

Fig. 10. (Matlab R2017a (9.2.0.538062)) The 3 dim, contour and line plots of $|\Psi_{11}(x, y, t)|$ $\sigma = 0.09, \zeta_1 = 10.5, \zeta_2 = 10.7, w = 5.7, k = 2, \lambda = 5.25, \theta = 0.02, \rho = -0.5, y = 1, z = 0$, and $\Xi(t) =$ randn.

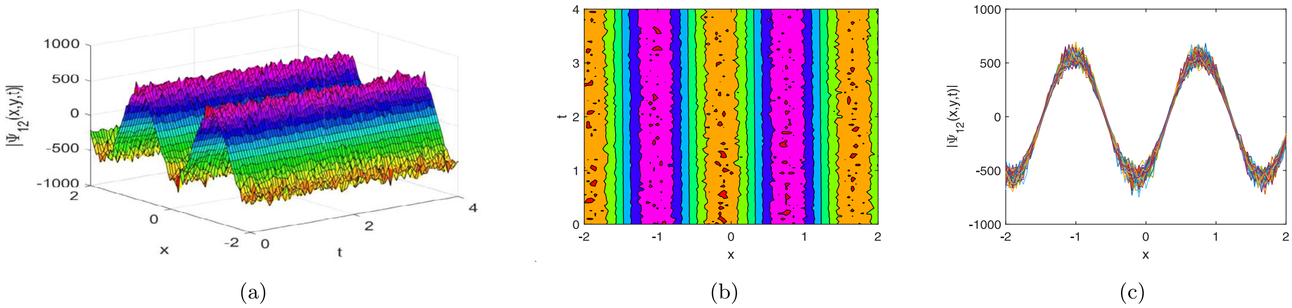

Fig. 11. (Matlab R2017a (9.2.0.538062)) The 3 dim, contour and line plots of $|\Psi_{12}(x, y, t)|$ $\sigma = 0.09, \zeta_1 = 10.5, \zeta_2 = 10.7, w = 6.7, k = 3.5, \lambda = 5.25, \theta = 0.02, \rho = -0.5, y = 1, z = 0$, and $\Xi(t) =$ randn.

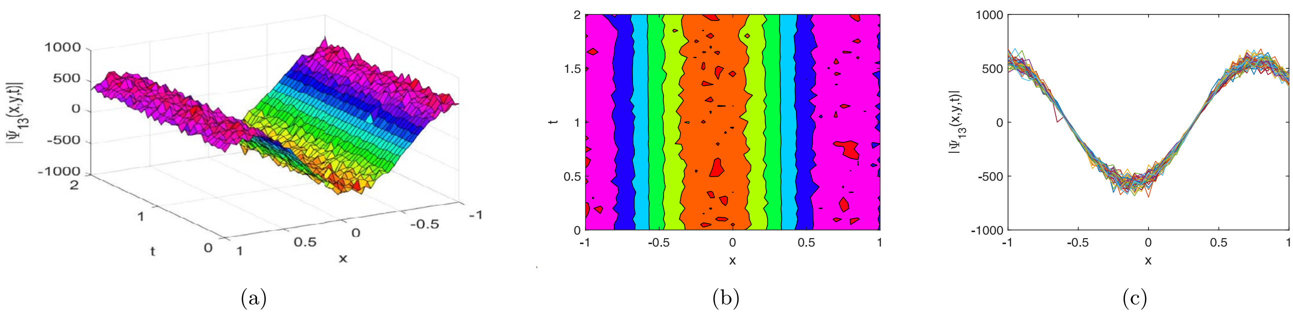

Fig. 12. (Matlab R2017a (9.2.0.538062)) The 3 dim, contour and line plots of $|\Psi_{13}(x, y, t)|$ $\sigma = 0.09, \zeta_1 = 10.5, \zeta_2 = 10.7, w = 6.7, k = 3.5, \lambda = 5.25, \theta = 0.02, \rho = 2.5, y = 1, z = 0$, and $\Xi(t) =$ randn.

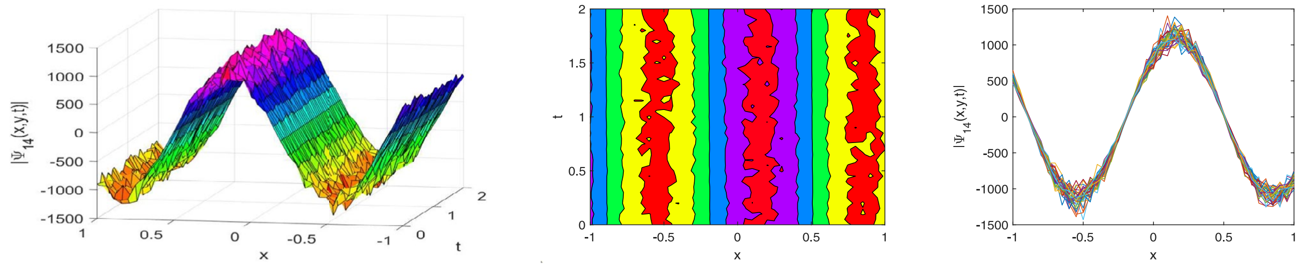

(a) (b) (c)

Fig. 13. (Matlab R2017a (9.2.0.538062)) The 3 dim, contour and line plots of $|\Psi_{14}(x,y,t)|$ $\sigma = 0.09, \zeta_1 = 10.5, \zeta_2 = 10.7, w = 8.7, k = 4.5, \lambda = 5.85, \theta = 0.02, \rho = 2.5, y = 1, z = 0$, and $\Xi(t) =$ randn.

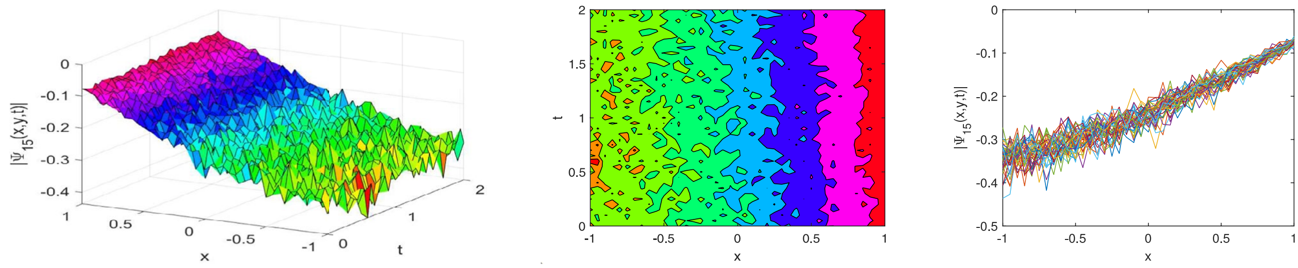

(a) (b) (c)

Fig. 14. (Matlab R2017a (9.2.0.538062)) The 3 dim, contour and line plots of $|\Psi_{15}(x,y,t)|$ $\sigma = 0.09, \zeta_1 = 10.5, \zeta_2 = 10.7, w = 8.7, k = 0.5, \lambda = 0.85, \theta = 0.02, \rho = 0, y = 1, z = 0$, and $\Xi(t) =$ randn.

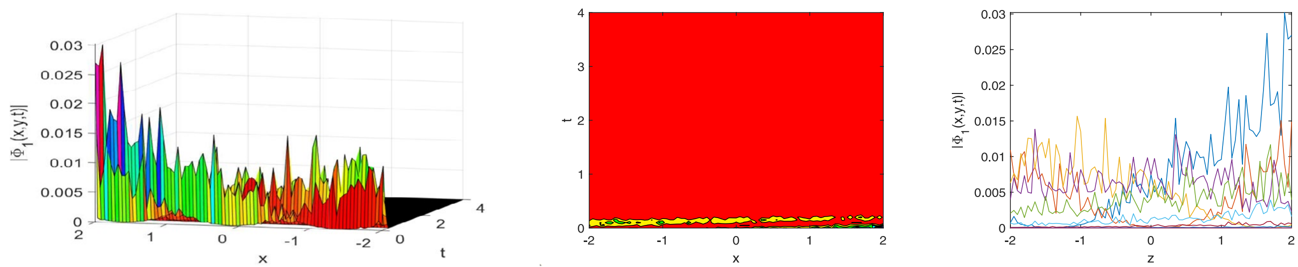

(a) (b) (c)

Fig. 15. (Matlab R2017a (9.2.0.538062)) The 3 dim, contour and line plots of $|\Phi_1(x,y,t)|$ for $\sigma = 0.09, \zeta_1 = 10.5, \zeta_2 = 10.7, w = 8.7, k = 0.5, \lambda = 0.85, \theta = 0.02, \rho = -190.6, y = 1, z = 0$, and $\Xi(t) =$randn.

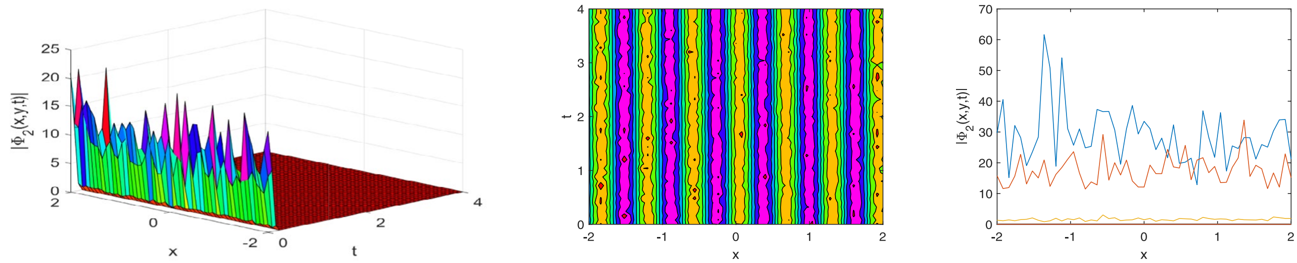

(a) (b) (c)

Fig. 16. (Matlab R2017a (9.2.0.538062)) The 3 dim, contour and line plots of $|\Phi_2\,(x, y, t)\,|$ for $\sigma = 0.06, \zeta_1 = 0.150, \zeta_2 = 1.7, w = 10.7, k = 5, \lambda = 0.125, \theta = 3.02, \rho = -190.6, y = 1, z = 0,$ and $\Xi(t)$ =randn.

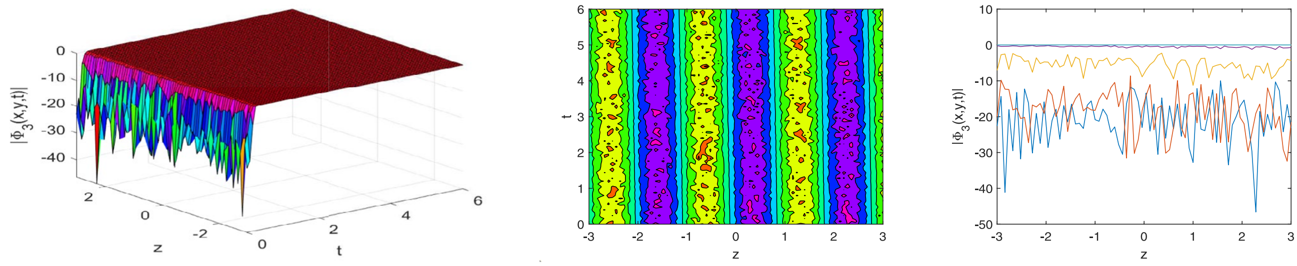

(a) (b) (c)

Fig. 17. (Matlab R2017a (9.2.0.538062)) The 3 dim, contour and line plots of $|\Phi_3\,(x, y, t)\,|$ for $\sigma = 0.08, \zeta_1 = 0.150, \zeta_2 = 1.70, w = 6.7, k = 2.63, \lambda = 2.25, \theta = 3.02, \rho = 125.6, y = 1, z = 0,$ and $\Xi(t)$ =randn.

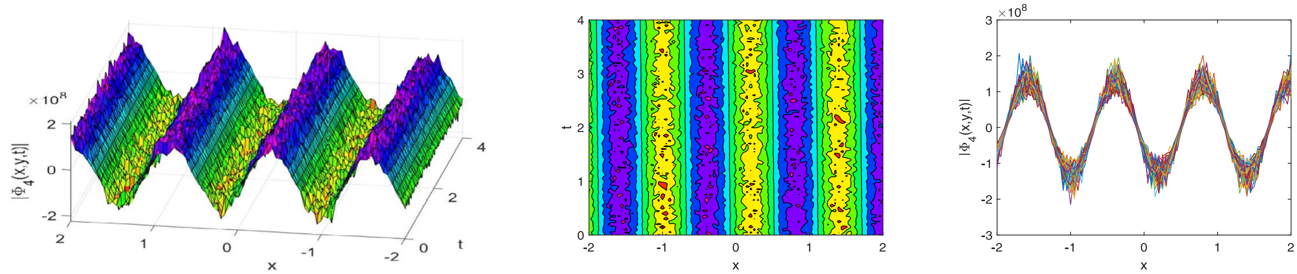

(a) (b) (c)

Fig. 18. (Matlab R2017a (9.2.0.538062)) The 3 dim, contour and line plots of $|\Phi_4\,(x, y, t)\,|$ for $\sigma = 0.09, \zeta_1 = 0.150, \zeta_2 = 1.7, w = 5.7, k = 2.63, \lambda = 10.25, \theta = 0.02, \rho = 2.06, y = 1, z = 0,$ and $\Xi(t)$ =randn.

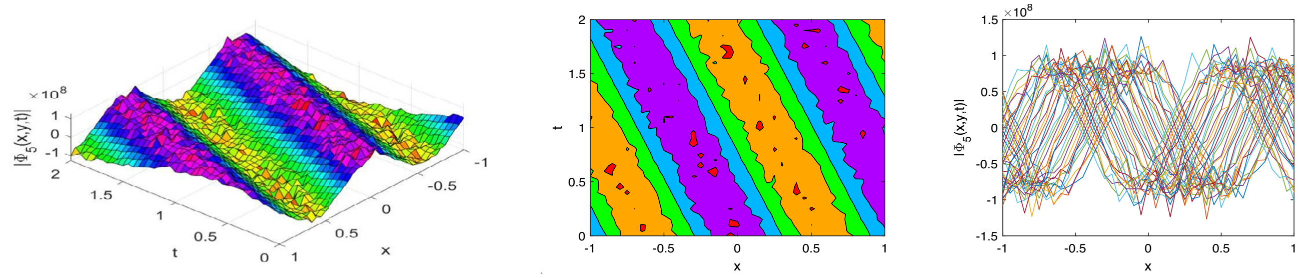

(a) (b) (c)

Fig. 19. (Matlab R2017a (9.2.0.538062)) The 3 dim, contour and line plots of $|\Phi_5\,(x,y,t)\,|$ for $\sigma=0.08, \zeta_1=0.150, \zeta_2=1.7, w=4.7, k=2.63, \lambda=10.25, \theta=1.02, \rho=0, y=1, z=0$, and $\Xi(t)=$ randn.

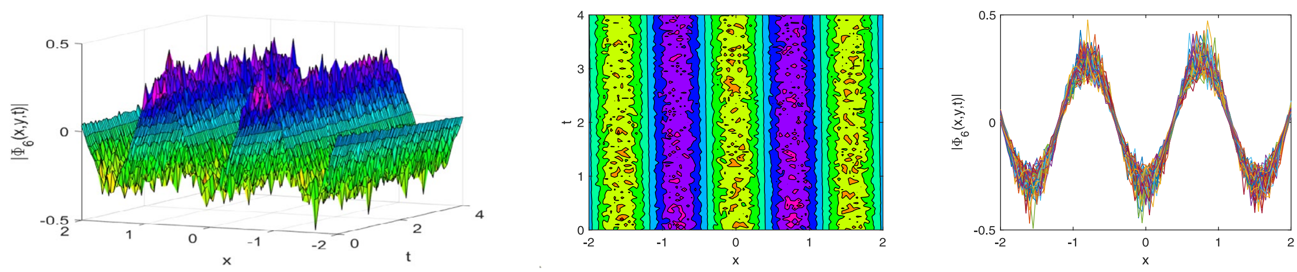

(a) (b) (c)

Fig. 20. (Matlab R2017a (9.2.0.538062)) The 3 dim, contour and line plots of $|\Phi_6\,(x,y,t)\,|$ for $\sigma=0.09, \zeta_1=10.50, \zeta_2=10.70, w=4.7, k=2, \lambda=2.25, \theta=0.02, \rho=-98825.5, y=1, z=0$, and $\Xi(t)=$randn.

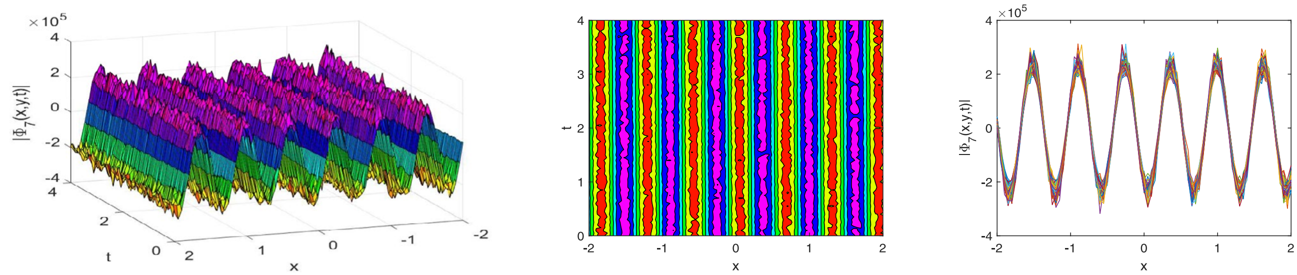

(a) (b) (c)

Fig. 21. (Matlab R2017a (9.2.0.538062)) The 3 dim, contour and line plots of $|\Phi_7\,(x,y,t)\,|$ for $\sigma=0.05, \zeta_1=-10.150, \zeta_2=10.70, w=10.7, k=5, \lambda=2.25, \theta=0.02, \rho=-10.5, y=1, z=0$, and $\Xi(t)=$randn.

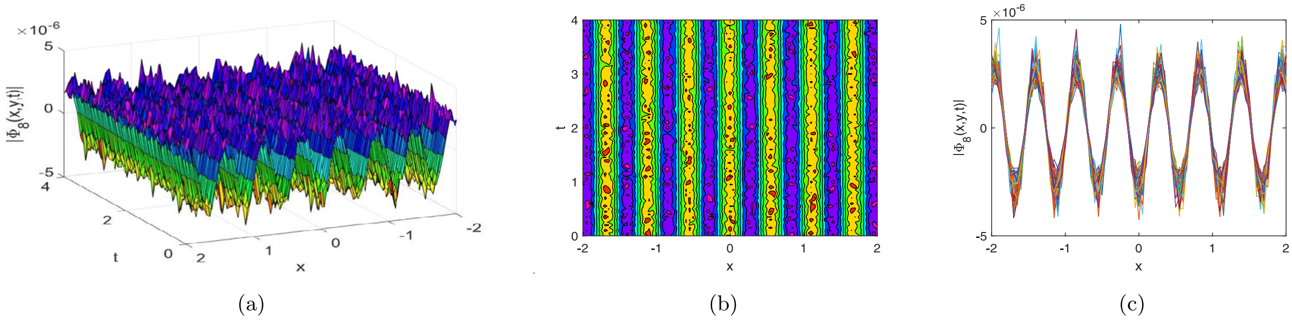

Fig. 22. (Matlab R2017a (9.2.0.538062)) The 3 dim, contour and line plots of $|\Phi_8\,(x, y, t)\,|$ for $\sigma = 0.09, \zeta_1 = 10.150, \zeta_2 = 3.7, w = 15.7, k = 5.63, \lambda = 0.025, \theta = 0.02, \rho = 98800, y = 1, z = 0$, and $\Xi(t)$ =randn.

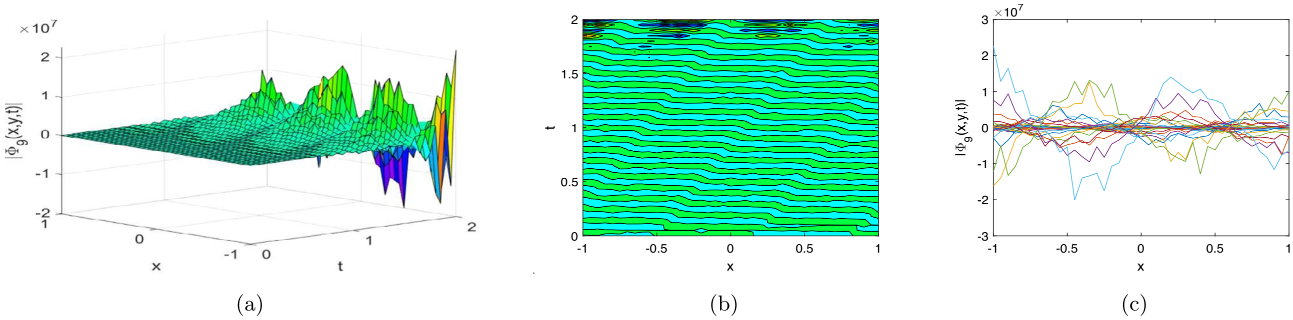

Fig. 23. (Matlab R2017a (9.2.0.538062)) The 3 dim, contour and line plots of $|\Phi_9\,(x, y, t)\,|$ for $\sigma = 0.16, \zeta_1 = 1.40, \zeta_2 = 1.80, w = 6.7, k = 2.35, \lambda = 1.025, \theta = 30.02, \rho = 0.0005, y = 1, z = 0$, and $\Xi(t)$ =randn.

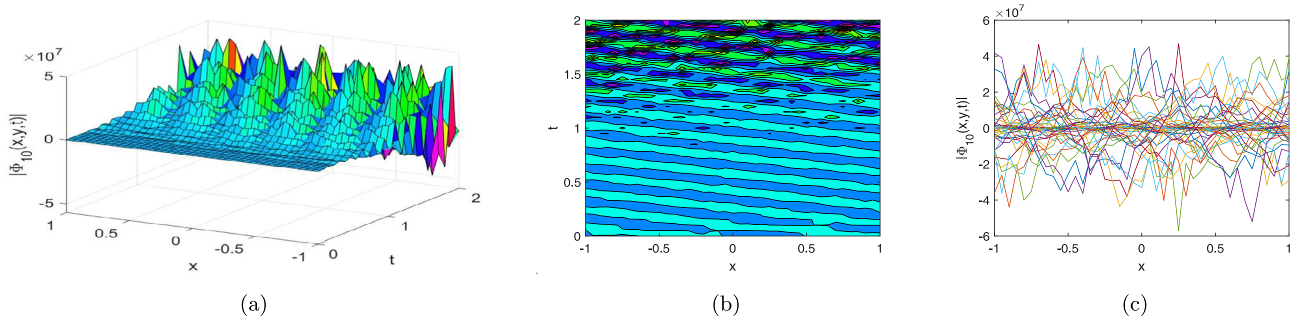

Fig. 24. (Matlab R2017a (9.2.0.538062)) The 3 dim, contour and line plots of $|\Phi_{10}\,(x, y, t)\,|$ for $\sigma = 0.16, \zeta_1 = 2.40, \zeta_2 = 2.80, w = 10.7, k = 5.7, \lambda = 0.85, \theta = 20.02, \rho = 0, y = 1, z = 0$, and $\Xi(t) =$ randn.

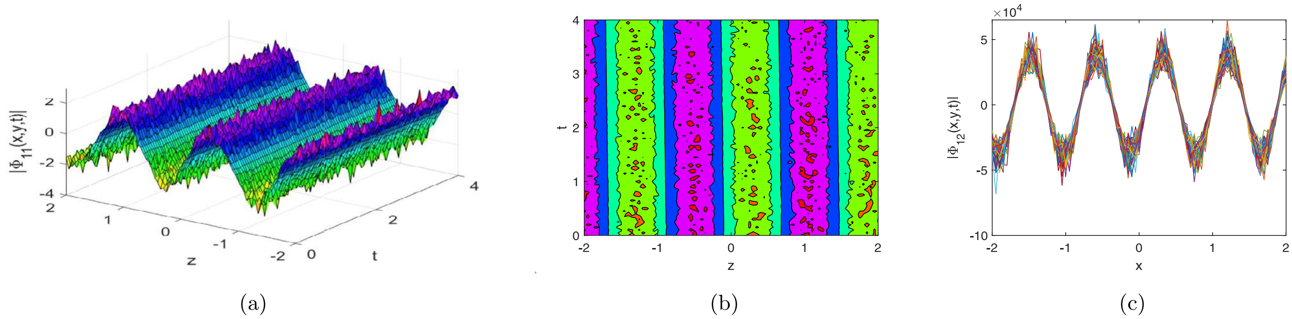

Fig. 25. (Matlab R2017a (9.2.0.538062)) The 3 dim, contour and line plots of $|\Phi_{11}(x, y, t)|$ for $\sigma = 0.09, \zeta_1 = 10.150, \zeta_2 = 10.70, w = 5.7, k = 2.0, \lambda = 2.25, \theta = 0.02, \rho = 0.02, y = 1, z = 0$, and $\Xi(t)$ =randn.

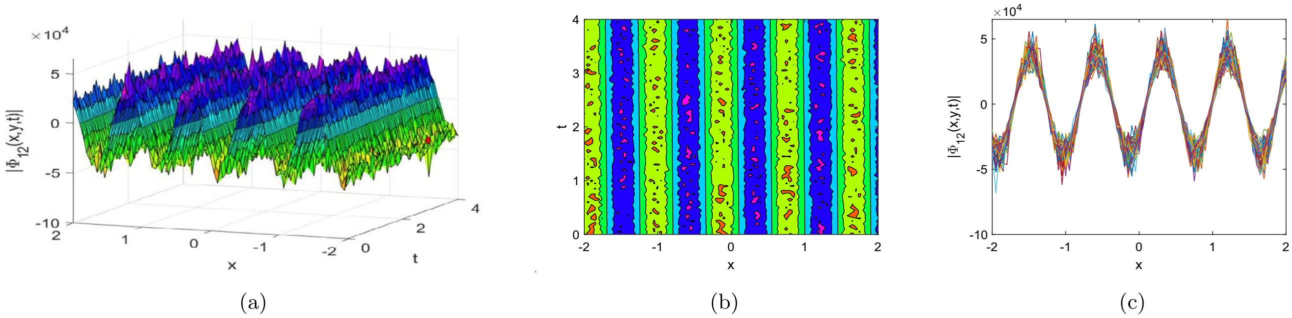

Fig. 26. (Matlab R2017a (9.2.0.538062)) The 3 dim, contour and line plots of $|\Phi_{12}(x, y, t)|$ for $\sigma = 0.09, \zeta_1 = 10.150, \zeta_2 = 10.70, w = 6.7, k = 3.5, \lambda = 5.25, \theta = 0.02, \rho - 0.5, y = 1, z = 0$, and $\Xi(t)$ =randn.

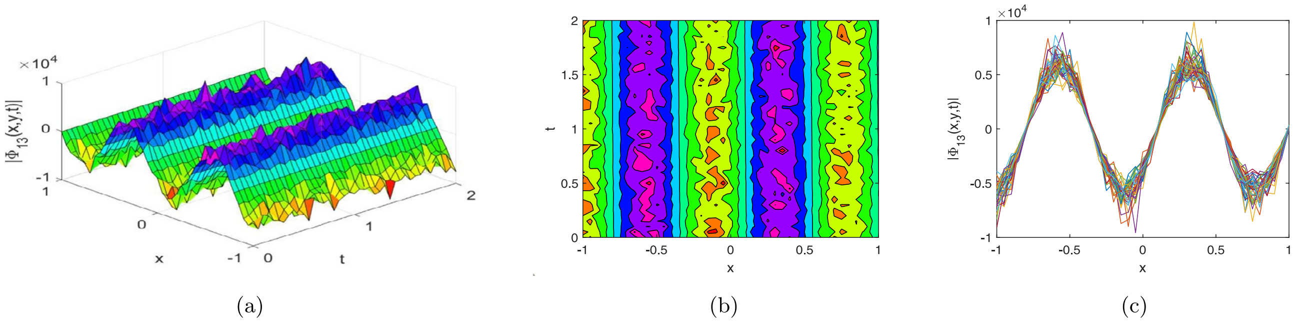

Fig. 27. (Matlab R2017a (9.2.0.538062)) The 3 dim, contour and line plots of $|\Phi_{13}(x, y, t)|$ for $\sigma = 0.06, \zeta_1 = 10.150, \zeta_2 = 10.70, w = 10.70, k = 3.5, \lambda = 5.25, \theta = 0.02, \rho = 2.5, y = 1, z = 0$, and $\Xi(t)$ =randn.

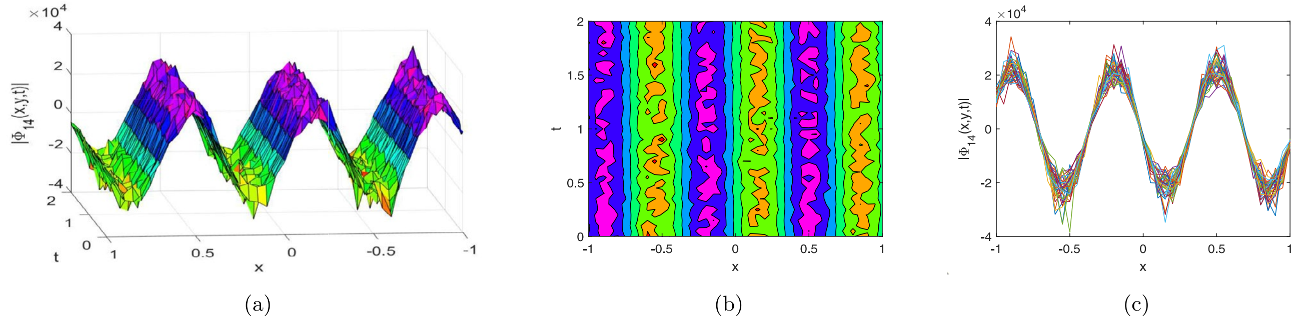

Fig. 28. (Matlab R2017a (9.2.0.538062)) The 3 dim, contour and line plots of $|\Phi_{14}(x,y,t)|$ for $\sigma = 0.09, \zeta_1 = 10.150, \zeta_2 = 10.70, w = 6.7, k = 6.7, \lambda = 5.25, \theta = 0.02, \rho = 2.5, y = 1, z = 0$, and $\Xi(t) =$randn.

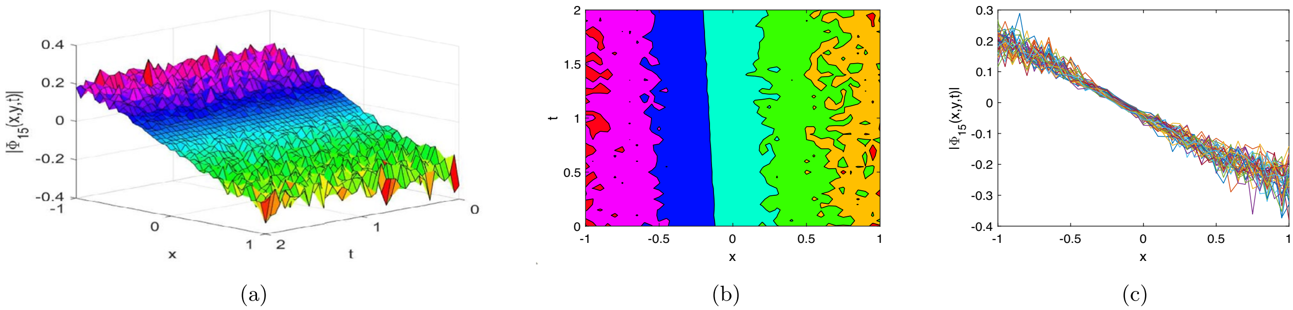

Fig. 29. (Matlab R2017a (9.2.0.538062)) The 3 dim, contour and line plots of $|\Phi_{15}(x,y,t)|$ for $\sigma = 0.09, \zeta_1 = 10.150, \zeta_2 = 10.70, w = 8.7, k = 0.5, \lambda = 0.85, \theta = 0.02, \rho = 0, y = 1, z = 0$, and $\Xi(t) =$ randn.

Data availability
All data generated or analyzed during this study are included in this article without any restrictions.

Received: 1 January 2025; Accepted: 19 May 2025
Published online: 25 May 2025

References
1. de Bouard, A. & Debussche, A. The stochastic nonlinear Schrödinger equation in H. (2003).
2. Raza, N., Sial, S. & Kaplan, M. Exact periodic and explicit solutions of higher dimensional equations with fractional temporal evolution. *Optik* **156**, 628–634 (2018).
3. Kaplan, M., Hosseini, K., Samadani, F. & Raza, N. Optical soliton solutions of the cubic-quintic non-linear Schrödinger‘s equation including an anti-cubic term. *J. Mod. Opt.* **65**(12), 1431–1436 (2018).
4. Raza, N., Jhangeer, A., Rahman, R. U., Butt, A. R. & Chu, Y. M. Sensitive visualization of the fractional Wazwaz–Benjamin–Bona–Mahony equation with fractional derivatives: A comparative analysis. *Results Phys.* **25**, 104171 (2021).
5. Arshed, S., Raza, N. & Alansari, M. Soliton solutions of the generalized Davey–Stewartson equation with full nonlinearities via three integrating schemes. *Ain Shams Eng. J.* **12**(3), 3091–3098 (2021).
6. Raza, N. & Arshed, S. Chiral bright and dark soliton solutions of Schrödinger‘s equation in (1+ 2)-dimensions. *Ain Shams Eng. J.* **11**(4), 1237–1241 (2020).
7. Guo, S. et al. Modulational stability and multiple rogue wave solutions for a generalized (3+ 1)-D nonlinear wave equation in fluid with gas bubbles. *Alex. Eng. J.* **106**, 1–18 (2024).
8. Pradhan, B. et al. Effect of trapping of electrons and positrons on the evolution of shock wave in magnetized plasma: A complex trapped K-dV burgers’ equation. *Results Phys.* **59**, 107617 (2024).
9. Gu, Y. et al. Bilinear method and semi-inverse variational principle approach to the generalized (2+ 1)-dimensional shallow water wave equation. *Results Phys.* **45**, 106213 (2023).
10. Wang, Z. et al. Wave propagation in finite discrete chains unravelled by virtual measurement of dispersion properties. *IET Sci. Meas. Technol.* **18**(6), 280–288 (2024).
11. Al-Askar, F. M., Cesarano, C. & Mohammed, W. W. Multiplicative Brownian motion stabilizes the exact stochastic solutions of the Davey–Stewartson equations. *Symmetry* **14**(10), 2176 (2022).
12. Mohammed, W. W., Al-Askar, F. M. & El-Morshedy, M. Impacts of Brownian motion and fractional derivative on the solutions of the stochastic fractional Davey–Stewartson equations. *Demo. Math.* **56**(1), 20220233 (2023).
13. Iqbal, M. S. & Inc, M. Optical Soliton solutions for stochastic Davey–Stewartson equation under the effect of noise. *Opt. Quant. Electron.* **56**(7), 1148 (2024).
14. Osborne, A. R. Modeling the Davey–Stewartson (DS) Equations. *Int. Geophys.* **97**, 867–875 (2010).
15. Aghdaei, M. F. & Manafian, J. Optical soliton wave solutions to the resonant Davey–Stewartson system. *Opt. Quant. Electron.* **48**, 1–33 (2016).

16. El-Shiekh, R. M. & Gaballah, M. Solitary wave solutions for the variable-coefficient coupled nonlinear Schrödinger equations and Davey–Stewartson system using modified sine-Gordon equation method. *J. Ocean Eng. Sci.* **5**(2), 180–185 (2020).
17. Günerhan, H. Optical soliton solutions of nonlinear Davey–Stewartson equation using an efficient method. *Rev. Mexic. Física* **67**(6), 1–10 (2021).
18. Hussain, S., Iqbal, M. S., Ashraf, R., Inc, M. & Tarar, M. A. Exploring nonlinear dispersive waves in a disordered medium: An analysis using ϕ^6 model expansion method. *Opt. Quant. Electron.* **55**(7), 651 (2023).
19. Mohammed, W. W., Al-Askar, F. M. & El-Morshedy, M. Impacts of Brownian motion and fractional derivative on the solutions of the stochastic fractional Davey–Stewartson equations. *Demo. Math.* **56**(1), 20220233 (2023).
20. Hussain, S. et al. Quantum analysis of nonlinear optics in Kerr affected saturable nonlinear media and multiplicative noise: A path to new discoveries. *Opt. Quant. Electron.* **55**(7), 578 (2023).
21. Gassem, F. et al. A novel approach to construct optical solitons solutions of complex Ginzburg–Landau equation with five distinct forms of nonlinearities. *Alex. Eng. J.* **113**, 551–564 (2025).
22. Hamza, A. E. et al. Soliton solutions and chaotic dynamics of the ion-acoustic plasma governed by a (3+ 1)-dimensional generalized Korteweg–de Vries–Zakharov–Kuznetsov equation. *Fract. Fract.* **8**(11), 673 (2024).
23. Lu, W., Ahmad, J., Akram, S. & Aldwoah, K. A. Soliton solutions and sensitive analysis to nonlinear wave model arising in optics. *Phys. Scr.* **99**(8), 085230 (2024).
24. Alqahtani, A. M., Akram, S., Ahmad, J., Aldwoah, K. A. & Rahman, M. U. Stochastic wave solutions of fractional Radhakrishnan–Kundu–Lakshmanan equation arising in optical fibers with their sensitivity analysis. *J. Opt.* **1**, 1–23 (2024).
25. Minier, J. P. & Chibbaro, S. Mathematical background on stochastic processes. In *Stochastic Methods in Fluid Mechanics* 1–38 (Springer, 2014).
26. Oksendal, B. *Stochastic Differential Equations: An Introduction with Applications* (Springer, 2013).
27. Karatzas, I. & Shreve, S. *Brownian Motion and Stochastic Calculus* Vol. 113 (Springer, 1991).
28. Revuz, D. & Yor, M. *Continuous Martingales and Brownian Motion* Vol. 293 (Springer, 2013).
29. Younas, U., Sulaiman, T. A., Ismael, H. F., Ren, J. & Yusuf, A. The study of nonlinear dispersive wave propagation pattern to Sharma–Tasso–Olver–Burgers equation. *Int. J. Mod. Phys. B* **38**(08), 2450112 (2024).
30. Younas, U., Yao, F., Nasreen, N., Khan, A. & Abdeljawad, T. Dynamics of M-truncated optical solitons and other solutions to the fractional Kudryashov's equation. *Results Phys.* **58**, 107503 (2024).
31. Younas, U., Sulaiman, T. A., Ren, J. & Yusuf, A. On the interaction phenomena to the nonlinear generalized Hietarinta-type equation. *J. Ocean Eng. Sci.* **9**(1), 89–97 (2024).
32. Younas, U. et al. A diversity of patterns to new (3+ 1)-dimensional Hirota bilinear equation that models dynamics of waves in fluids. *Results Phys.* **54**, 107124 (2023).
33. Yusuf, A., Alshomrani, A. S., Sulaiman, T. A., Younas, U. & Baleanu, D. On the breather waves, lump solutions, two-wave solutions of (3+ 1) dimensional Martínez Alonso–Shabat equation. *J. Ocean Eng. Sci.* (2022).
34. Younas, U. et al. Dynamics of optical wave profiles to the fractional three-component coupled nonlinear Schrödinger equation. *Fractals* **32**(05), 1–13 (2024).
35. Younas, U., Rezazadeh, H. & Ren, J. Dynamics of optical pulses in birefringent fibers without four-wave mixing effect via efficient computational techniques. *J. Ocean Eng. Sci.* (2022).
36. Manafian, J. & Lakestani, M. A new analytical approach to solve some of the fractional-order partial differential equations. *Indian J. Phys.* **91**, 243–258 (2017).
37. Hamali, W., Manafian, J., Lakestani, M., Mahnashi, A. M. & Bekir, A. Optical solitons of M-fractional nonlinear Schrödinger's complex hyperbolic model by generalized Kudryashov method. *Opt. Quant. Electron.* **56**(1), 7 (2024).
38. Juadih, W. R. et al. On traveling wave solutions for the transmission line model of nano-ionic currents along MTs arising in nanobiosciences. *Opt. Quant. Electron.* **56**(4), 635 (2024).
39. Gui, X. C. et al. Wave pulses' physical properties in birefringent optical fibers containing two vector solitons with coupled fractional LPD equation with Kerr's law nonlinearity. *Opt. Quant. Electron.* **56**(6), 913 (2024).
40. Islam, W. & Younis, M. Weakly nonlocal single and combined solitons in nonlinear optics with cubic quintic nonlinearities. *J. Nanoelectron. Optoelectron.* **12**(9), 1008–1012 (2017).
41. Younis, M. et al. Analytical optical soliton solutions of the Schrödinger–Poisson dynamical system. *Results Phys.* **27**, 104369 (2021).
42. Hubert, M. B. et al. Optical solitons with Lakshmanan–Porsezian–Daniel model by modified extended direct algebraic method. *Optik* **162**, 228–236 (2018).
43. Soliman, A. A. The modified extended direct algebraic method for solving nonlinear partial differential equations. *Int. J. Nonlinear Sci.* **6**(2), 136–144 (2008).
44. Soliman, A. A. & Abdo, H. A. New exact Solutions of nonlinear variants of the RLW, the PHI-four and Boussinesq equations based on modified extended direct algebraic method. http://arxiv.org/abs/1207.5127. (2012).
45. Hubert, M. B. et al. Optical solitons with modified extended direct algebraic method for quadratic-cubic nonlinearity. *Optik* **162**, 161–171 (2018).
46. Hubert, M. B. et al. Optical solitons in parabolic law medium with weak non-local nonlinearity using modified extended direct algebraic method. *Optik* **161**, 180–186 (2018).
47. Samir, I., Badra, N., Ahmed, H. M. & Arnous, A. H. Solitons dynamics in optical metamaterial with quadratic-cubic nonlinearity using modified extended direct algebraic method. *Optik* **243**, 166851 (2021).
48. Ali, A. H. A. The modified extended tanh-function method for solving coupled MKdV and coupled Hirota-Satsuma coupled KdV equations. *Phys. Lett. A* **363**(5–6), 420–425 (2007).
49. Abdou, M. A. & Soliman, A. A. Modified extended tanh-function method and its application on nonlinear physical equations. *Phys. Lett. A* **353**(6), 487–492 (2006).
50. Zhuo-Sheng, L. & Hong-Qing, Z. On a new modified extended tanh-function method. *Commun. Theor. Phys.* **39**(4), 405 (2003).
51. Elwakil, S. A., El-Labany, S. K., Zahran, M. A. & Sabry, R. Modified extended tanh-function method and its applications to nonlinear equations. *Appl. Math. Comput.* **161**(2), 403–412 (2005).
52. Soliman, A. The modified extended tanh-function method for solving Burgers-type equations. *Physica A* **361**(2), 394–404 (2006).
53. Eldidamony, H. A., Ahmed, H. M., Zaghrout, A. S., Ali, Y. S. & Arnous, A. H. Highly dispersive optical solitons and other solutions in birefringent fibers by using improved modified extended tanh-function method. *Optik* **256**, 168722 (2022).
54. Sekulić, D. L., Satarić, M. V. & Živanov, M. B. Symbolic computation of some new nonlinear partial differential equations of nanobiosciences using modified extended tanh-function method. *Appl. Math. Comput.* **218**(7), 3499–3506 (2011).
55. Yan, X. W., Long, H. & Chen, Y. Prediction of general high-order lump solutions in the Davey–Stewartson II equation. *Proc. R. Soc. A* **479**(2280), 20230455 (2023).
56. Behera, S. & Virdi, J. P. Generalized soliton solutions to Davey–Stewartson equation. *Nonlinear Opt. Quant. Opt.* **57**(3–4), 325–337 (2023).
57. Ding, C. C., Zhou, Q., Triki, H., Sun, Y. & Biswas, A. Dynamics of dark and anti-dark solitons for the x-nonlocal Davey–Stewartson II equation. *Nonlinear Dyn.* **111**(3), 2621–2629 (2023).
58. Coppini, F., Grinevich, P. G. & Santini, P. M. The periodic N breather anomalous wave solution of the Davey–Stewartson equations; first appearance, recurrence, and blow up properties. *J. Phys. A* **57**(1), 015208 (2023).
59. Guo, B., Fang, Y. & Dong, H. Time-fractional Davey–Stewartson equation: Lie point symmetries, similarity reductions, conservation laws and traveling wave solutions. *Commun. Theor. Phys.* **75**(10), 105002 (2023).

60. Liu, C. & Li, Z. Multiplicative Brownian motion stabilizes traveling wave solutions and dynamical behavior analysis of the stochastic Davey–Stewartson equations. *Results Phys.* **53**, 106941 (2023).

Acknowledgements
The authors extend their gratitude to the Islamic University of Madinah. This study is supported via funding from Prince Sattam bin Abdulaziz University project number (PSAU/2025/R/1446).

Declarations

Competing interests
the authors declares no competing interests.

Additional information
Correspondence and requests for materials should be addressed to M.A.A. or K.A.A.

Reprints and permissions information is available at www.nature.com/reprints.

Publisher's note Springer Nature remains neutral with regard to jurisdictional claims in published maps and institutional affiliations.

Open Access This article is licensed under a Creative Commons Attribution-NonCommercial-NoDerivatives 4.0 International License, which permits any non-commercial use, sharing, distribution and reproduction in any medium or format, as long as you give appropriate credit to the original author(s) and the source, provide a link to the Creative Commons licence, and indicate if you modified the licensed material. You do not have permission under this licence to share adapted material derived from this article or parts of it. The images or other third party material in this article are included in the article's Creative Commons licence, unless indicated otherwise in a credit line to the material. If material is not included in the article's Creative Commons licence and your intended use is not permitted by statutory regulation or exceeds the permitted use, you will need to obtain permission directly from the copyright holder. To view a copy of this licence, visit http://creativecommons.org/licenses/by-nc-nd/4.0/.

© The Author(s) 2025